Quasi Z source direct matrix converter based K- to three-phase wind energy conversion system using maximum constant boost current control modulation technique

Mani Karthick, Venkatasalam Rukkumani & Soundarapandiyan Manivannan

Published online: 08 Aug 2024.

Submit your article to this journal ⬈

Article views: 283

View related articles ⬈

View Crossmark data ⬈

Quasi Z source direct matrix converter based K- to three-phase wind energy conversion system using maximum constant boost current control modulation technique

Mani Karthick[a], Venkatasalam Rukkumani[b] and Soundarapandiyan Manivannan [c]

[a]Park College of Engineering and Technology, Coimbatore, India; [b]Sri Ramakrishna Engineering College, Coimbatore, India; [c]SRM Institute of Science and Technology, Ramapuram, Chennai

ABSTRACT

The conversion system for wind energy has no restriction on the number of output phases. K numbers of output phases can be converted into standard grid-connected three-phase supply using a quasi-Z source direct matrix converter (QZSDMC). The obtained input supply may be five phases from the wind energy conversion system with continuously variable frequency as well as variable terminal voltages. Using the proposed QZSDMC converter with maximum constant boost current control modulation technique constant three-phase voltages as well as frequency can be maintained at the grid side. Additionally, the energy conversion system has high output voltage gain. The proposed converter as well as the modulation technique produces the maximum voltage transfer ratio of 1.05. The output voltage gain reached nearly 1.99 compared with the traditional power converters. The voltage THD and current THD are maintained within the acceptable limit of 5.3 and 3.6 respectively. The power factor have been maintained nearly unity throughout the all mode of operations. To stabilize the grid frequencies and grid voltages additional control blocks are used. This research article presents simulation results for the proposed QZSDMC converter with a maximum constant boost current control modulation technique. Also, the proposed scheme has been validated with suitable experimental results.

1. Introduction

Wind Energy is the amount of kinetic energy that exists in the moving air. The available kinetic energy from the wind is converted into electrical power with the help of a wind turbine coupled to an electrical generator. In a classic wind turbine, the Kinetic Energy of Wind is converted into rotational motion by rotor assemblies with three blades at the front of the wind turbine. After the conversion of mechanical energy from the wind into electrical energy by the generator, the produced AC power is supplied to standalone AC loads or the grid with the help of an integrated power converter [1]. Owing to the variation in wind speed, the output parameters of the generator also fluctuate. But mostly all the electrical loads operate at fixed voltage and frequency. By utilizing power converters in WECS, the performance of the wind turbine can be enhanced, and the desired output can also be delivered. Hence, various power converter topologies for PMG-based WECS have been explored to provide low-cost and highly efficient power conversion [2].

Power converters play a predominant role in the variable speed Wind Energy Conversion System since it serves as the conditioning interference between the generator and load. A simple low-cost arrangement consisting of a diode rectifier, a boost chopper, and a voltage source inverter has been proposed in [3]. Two level back-to-back power converters are also presented in [4]. The introduction of a two-stage conversion with a diode rectifier coupled with a Z-Source Inverter has been proposed in [5]. Later, a three-level back-to-back Neutral Point Converter (NPC) has also been discussed by [6]. A power converter integrating a diode rectifier, a three-level boost converter, and an NPC inverter for interfacing the generator output to the grid have been proposed in[7]. In recent years, the utilization of Matrix Converter as the grid interface between PMSG and WECS has gained more attention as presented by [8].

Quasi Z-Source Inverters (qZSI) have emerged as a promising solution for addressing the limitations of traditional inverters in power conversion applications. This literature review provides a comprehensive overview of the theory, applications, recent advancements, and future prospects of qZSI technology. The qZSI concept originated from the traditional Z-Source Inverter (ZSI), which utilizes an impedance network to boost voltage levels and provide buck–boost capabilities [2]. Unlike conventional inverters, qZSI employs a quasi-Z network with additional features, such as

reduced component count, improved efficiency, and enhanced reliability. The unique topology of qZSI allows bidirectional power flow, reduced electromagnetic interference, and increased flexibility in voltage regulation [3].

The qZSI technology finds applications across various industries, including renewable energy systems, electric vehicles, grid-tied inverters, and uninterruptible power supplies. In renewable energy systems, qZSI enables integration with solar panels and wind turbines, offering improved efficiency and grid stability [4]. Electric vehicles benefit from qZSI's compact design, high power density, and regenerative braking capabilities, enhancing overall performance and range. Grid-tied inverters equipped with qZSI support grid stabilization, voltage regulation, and power quality improvement, facilitating the integration of renewable energy sources into the electrical grid. Additionally, qZSI-based uninterruptible power supplies provide reliable backup power solutions for critical infrastructure, data centres, and industrial applications [5].

Recent research efforts have focused on enhancing the performance, efficiency, and reliability of qZSI technology. Advanced control algorithms, such as predictive control, model predictive control, and artificial intelligence-based techniques, have been proposed to optimize qZSI operation under varying load conditions and grid disturbances. Moreover, innovative modulation strategies, such as space vector modulation, pulse width modulation, and hybrid modulation techniques, have been investigated to minimize harmonic distortion, improve transient response, and reduce switching losses in qZSI-based systems. Furthermore, advancements in semiconductor devices, passive components, and thermal management techniques have contributed to the miniaturization, cost reduction, and reliability enhancement of qZSI implementations [6].

Despite significant progress, several challenges remain to be addressed in the development and deployment of qZSI technology. These include the optimization of control strategies for multi-level qZSI topologies, the integration of energy storage systems for grid support applications, and the standardization of testing procedures and performance metrics. Future research directions may focus on addressing these challenges while exploring emerging applications, such as microgrids, smart cities, and electrified transportation systems. Additionally, efforts to improve the manufacturability, scalability, and cost-effectiveness of qZSI solutions will be critical for widespread adoption in real-world applications [7].

The extended Z-Source concept to explore a family of Z-Source Matrix Converters (ZSMC) have been developed by [8]. The principle, features, and boost control of voltage fed ZSMC has been analyzed. A new improved modulation for intermediate ZSMC has been proposed by [9]. A Z-Source impedance network has been inserted to the fictitious dc link of indirect MC. Later on, a three phase indirect matrix converter with two ZS networks have been proposed. This paper recommends a novel arrangement of two ZS networks with a MC to achieve a very high voltage gain for integrating renewable energy sources to grid. However, the disadvantages of Z-Source Inverter include limited voltage boost ratio and associated phase shift that makes the control inaccurate [10]. The comparative evaluation of three phase ZS/QZS IMC have been investigated. ZS and QZS circuits of current DMCs are employed for an IMC topology to increase voltage gain and simplify commutation but they still require additional input filter [11]. Omar et al. have compared conventional matrix converter with new Quasi Z-Source Direct Matrix Converter, which provides buck boost function by introducing a Z-Source concept. Mojtaba Alizadeh et al. have proposed a quasi-Z source matrix converter which consists of three phase quasi ZS network followed by a MC, as grid interface of PMSG based WECS [12].

The wind's erratic behaviour means that the PMG output voltage and frequency will fluctuate over time. Power conditioning circuits are necessary to enable the regulation of the DDWECS's terminal voltage and frequency. Conventional three-stage conversion results in higher THD, decreased efficiency, and significant switching stress. In addition, the matrix converter's low voltage transfer ratio of 0.866, higher control complexity, intricate commutation techniques, and sensitivity to input voltage perturbations are issues in single stage conversion. Recently, ZSDMC has been proposed to allow short circuits and facilitate commutation. However, ZSDMC's drawbacks include a low voltage transfer ratio, imprecise control, and irregular input current [13].

To improve the voltage transfer ratio, new continuous QZSDMC and QZSIMC have been proposed in this study. Without compromising the converter's efficiency, the duty ratio of the quasi-Z source network can be raised by adjusting the shoot through distribution in space vector modulation. This raises the boost factor of QZSMC. Higher voltage gain, less switching voltage and current stress, and constant input current are thus offered by the suggested QZSMC [14]. This research article has been organized as; Section II represents a detailed explanation of the matrix converter and its evoluation. Section III represents a detailed explanation of the maximum constant boost current control modulation practice followed by Section IV denotes the concept evaluation by doing the MATLAB simulation. Section V consists of experimental validation followed by an assessment of the proposed modulation scheme and topology with previous topologies. Section VI gives the proper conclusion to this research article.

2. Matrix converter topologies

A Matrix Converter as shown in Figure 1 is an advanced power electronic device used for the direct conversion of electrical energy between alternating current (AC) systems, typically without the prerequisite for intermediate energy storage or additional apparatuses like DC-link capacitors [15]. Unlike traditional converters which use rectifiers and inverters separately, a matrix converter can directly convert AC to AC with variable voltage and frequency, offering greater efficiency and flexibility [16]. Matrix converters are acknowledged for their ability to precisely control AC power and have applications in various industries, including motor drives, renewable energy systems, and aerospace [17]. They are highly regarded for their compact size, improved power quality, and reduced energy losses, making them a valuable asset in modern power electronics [18].
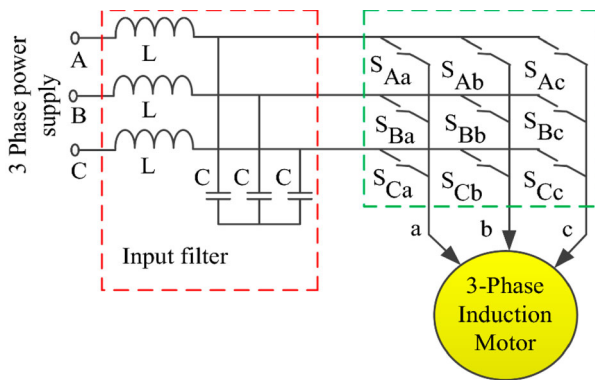

Figure 1. Traditional direct matrix converter.

The Impedance-Source Direct Matrix Converter (ISDMC) as revealed in Figure 2 is a novel and sophisticated power electronics system that combines the principles of impedance-source inverters with matrix converters. This innovative technology provides a versatile solution for electrical energy transfiguration [19]. Unlike traditional voltage source or current source inverters, the ISMC offers inherent impedance-adaptability, bidirectional power flow, and minimized harmonic distortions. These features make it highly suitable for various solicitations, including renewable energy assimilation, motor drives, and power dissemination systems. The ISMC's unique design and control capabilities make it a promising solution for enhancing energy conversion efficiency and grid compatibility in modern electrical systems [20].

The QZSDMC as shown in Figure 3 is an innovative power electronic system designed for efficient and flexible energy conversion. Combining the advantages of quasi-Z-source and direct matrix converter technologies, it enables bidirectional energy flow with minimal harmonic distortion, making it suitable for various solicitations, including renewable energy assimilation, electric vehicle charging, and industrial processes. The QZSDMC's unique topology offers superior control and power quality, making it a promising solution for the evolving energy landscape [21].

This exploration article introduces the Voltage-Fed QZSDMC, depicted in Figure 4. It is designed for the conversion of five-phase to three-phase power, employing the Maximum Constant Boost Current Control Modulation technique. To enhance efficiency and mitigate switching losses, a novel PWM approach is proposed, governing both the rectifier and inverter
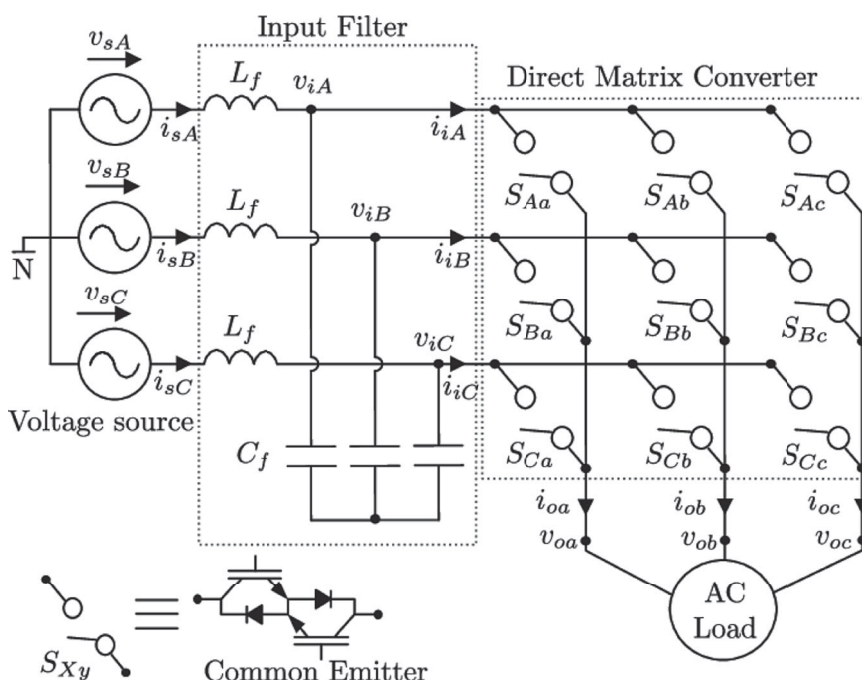

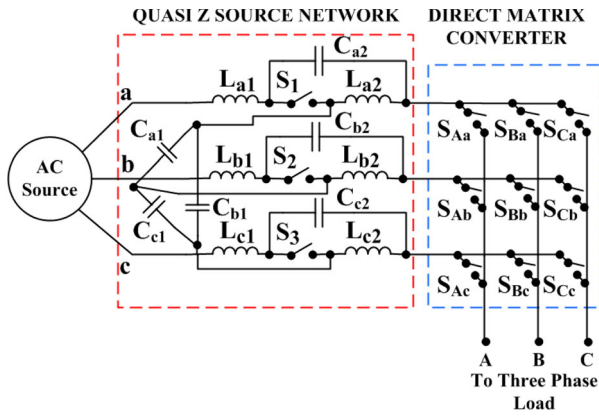**Figure 2.** Impedance-source direct matrix converter.

Figure 3. Quasi-Z-source direct matrix converter.

3. Maximum constant boost current control modulation technique

This subdivision focuses on the practical application of the Maximum Constant Boost Current Control Modulation technique for the conversion of five-phase to three-phase power using the QZSDMC. When using this control method [23], the maximum and minimum appropriate DC link voltages for the matrix converter serve as the upper and lower envelopes obtained from the five-phase input waveform, directing the transition of output phase voltages. The "zero output voltage changeover state" refers to the situation where all three output phase controls are coupled to identical input phases in the framework of the QZSDMC. In this condition, the shoot-through voltage used as a reference must be either greater or lower than the maximum or lowest carrier voltage since all three outcomes phase voltages are more than or below the carrier voltage [24, 25].

The control method employs two straight lines, one defining the upper limit and the other the lower limit, to enclose the maximum and minimum reference voltage envelope. Although the modulation index remains constant for specific reference voltages, the shoot-through duty ratio varies over time. Compared to the straightforward boost control utilized in the Z-source inverter, this control technique is rather different [26]. Within the QZSDMC, two sets of bidirectional switches are at your disposal. The first set (S0) manages the activation or deactivation of the impedance source network connected to the matrix converter, while the second set (S1–S15) connects the load terminals to the source, similar to a conventional matrix converter.
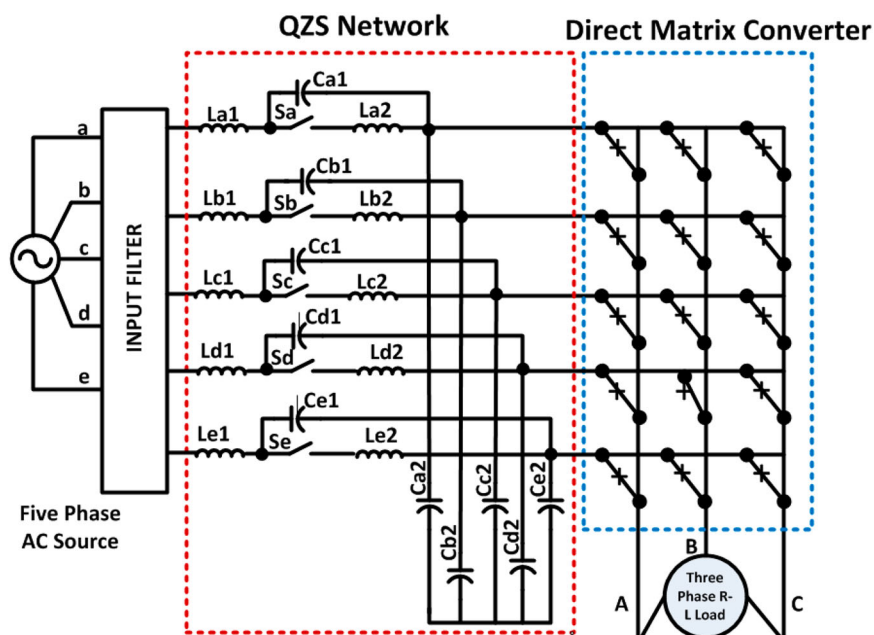
sides of the matrix converter's equivalent circuit. In comparison to the Z Source Dual Matrix Converter (ZSDMC), the Voltage-Fed QZSDMC offers advantages such as reduced component count, compactness, heightened efficiency, and a broad operational range for buck–boost conversion [22]. The newly suggested modulation technique yields several benefits, including reduced output harmonic content, diminished switching current stresses, maximum voltage gain, and lower switching voltages within the given modulation index range. This article conducts an in-depth exploration of the interplay between voltage gain and modulation index, as well as the correlation between switching voltage stresses and voltage gain. The proposed modulation technique's efficacy is validated through simulation using MATLAB and experimentation, demonstrating its practical utility.

Figure 4. Proposed voltage-fed quasi-Z-source direct matrix converter.

In the shoot-through condition, (S0) is simultaneously disabled while all output phase controls in the typical matrix converter are turned on and connected to the same input leg switches. The status of switch (S0) will remain on for a prolonged shoot-through period, and the other switches are managed similarly to a traditional matrix converter. The voltage boost ratio value is determined using the volt-second balance equation based on the Z-source inductor. The average voltage across the inductor in the Z-source network approximates zero over one switching period, with the minor fundamental voltage drop neglected due to the significant difference in switching frequency compared to the fundamental frequency [27].

To harness the shoot-through states for voltage boost, PWM control for the traditional matrix converter must undergo modification. An additional shoot-through reference is required to be designed for comparison with the carrier waveform, generating an extra shoot-through signal [28]. This concept can be adapted from control methods utilized in the Z-source inverter. Two distinct approaches are proposed: "Simple Maximum Boost Control", which inherits the straight lines of simple boost control, and "Maximum Constant Boost Current Control", which maximizes the utilization of zero states while maintaining a constant shoot-through duty ratio. The analysis indicates that for voltage gains below 0.866, no shoot-through state is required to maintain minimal voltage and current stress on the devices. However, for voltage gains exceeding 0.866, Maximum Constant Boost Current Control can significantly reduce output harmonics due to its time-invariant shoot-through duty ratio [29].

The third harmonic injection is used to get a modulation index of 0.866. The third harmonic injection enables the modulation index to reach 0.866 as opposed to the prior method's cap of 0.5. As seen by the dotted line in Figure 5, this involves introducing a triangular third-harmonic voltage into the recommendations which are analogous to the space vector PWM approach. The suggested third harmonic injection technique is shown in Figure 5. MAX and MIN of Figure 5 have been changed to (MX-MN) and 0, respectively, in this rendering. The three-phase output comparison voltages are effectively constrained inside this envelope since the carrier signal is encompassed within this (MX-MN), guaranteeing that they never go above the carrier voltage. The reference voltages VoA, VoB, and VoC are the results of the third harmonic injection [30].

Assume that the five-phase input voltages and three-phase output reference voltages are:

$$\begin{bmatrix} V_{OA} \\ V_{OB} \\ V_{OC} \end{bmatrix} = V_{om} \begin{bmatrix} sin(w_i t) \\ sin\left(w_o t - \dfrac{2\pi}{3}\right) \\ sin\left(w_o t + \dfrac{2\pi}{3}\right) \end{bmatrix} \quad (1)$$

$$\begin{bmatrix} V_a \\ V_b \\ V_c \\ V_d \\ V_e \end{bmatrix} = V_{im} \begin{bmatrix} sin(w_i t + \alpha) \\ sin\left(w_i t + \alpha - \dfrac{2\pi}{5}\right) \\ sin\left(w_i t + \alpha - \dfrac{4\pi}{5}\right) \\ sin\left(w_i t + \alpha + \dfrac{4\pi}{5}\right) \\ sin\left(w_i t + \alpha + \dfrac{2\pi}{5}\right) \end{bmatrix} \quad (2)$$

The maximum modulation index can reach 0.866. The injected third harmonic expression is:

$$V_{0ref\_3} = (MAX(V_{0A}^*, V_{0B}^*, V_{0C}^*) + MIN(V_{0A}^*, V_{0B}^*, V_{0C}^*))/2 \quad (3)$$

Where, V_{0A}^*, V_{0B}^*, V_{0C}^* are the original sinusoidal three-phase output voltage references. Va, Vb, Vc, Vd, and Ve are the original sinusoidal three-phase output voltage references [31].
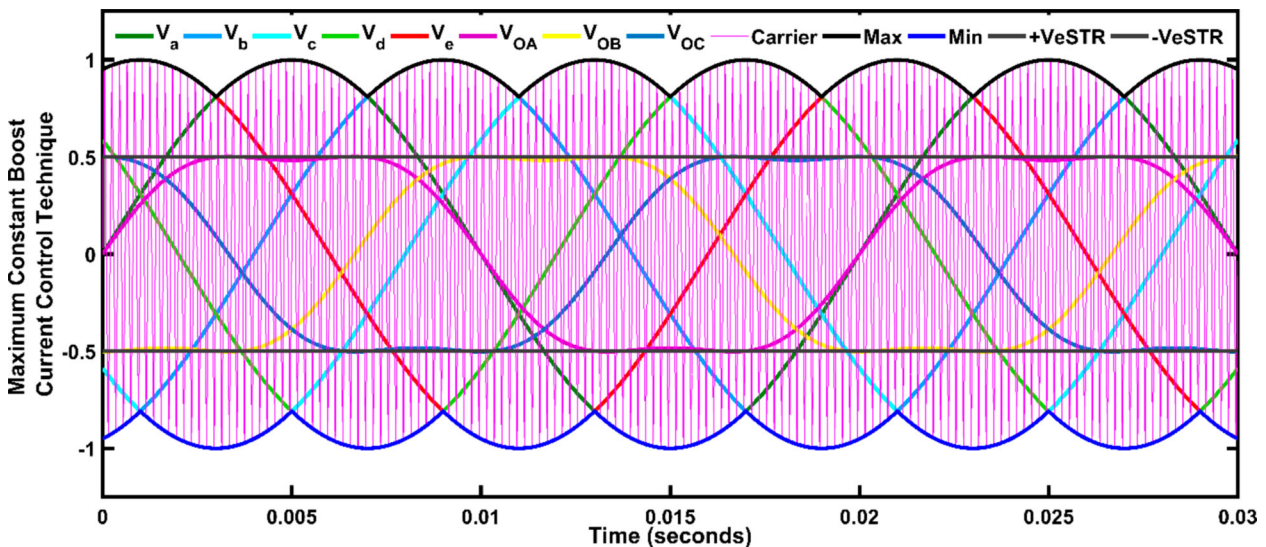

Figure 5. Maximum constant boost current control technique.

This approach aligns with the Space Vector Pulse Width Modulation technique. In the case of Simple Maximum Boost Control, a linear reference line is used to connect the upper and lower envelopes of the output reference. All zero states are used by Maximum Boost Current Control as the shoot-through state, which causes its shoot-through reference to overlap with both the lower and the upper output voltage envelopes [32–34]. Even at its highest value, Maximum Constant Boost Current Regulation maintains a constant shoot-through duty ratio. To establish the link between voltage gain and modulation index for operational parameter design, the shoot-through duty cycle may be calculated as a function of the modulation index. In each method, the magnitude of the shoot-through reference is used to calculate the shoot-through duty cycle. The Instantaneous Duty Ratio $D0(t)$ in the Maximum Boost Current Management approach is not a periodic function, in contrast to the Simple Boost Control technique. This modulation technique is applied in the QZSDMC, where it manages various input and output three-phase voltages and currents [35–37].

The inclusion of shoot-through situations in the quasi-Z source system is shown in Figure 6. The emergence of the shoot-through switching state is achieved through the comparison of the original carrier signal with the output standard modulating signals when all three-phase flipping signals are in either the high or low states. When the carrier triangle signal exceeds or deviates from the three-phase baseline output modulating signals, the shoot-through signal is produced. Short circuits and storage of energy in capacitors and inductors inside a quasi-impedance system are permitted as a result of using shoot-through states during this time. This stored energy is subsequently utilized during the through period, resulting in a significant boost to the output [38].

The momentary shoot-through duty ratio is determined using the maximum constant boost current regulation approach as:

$$D_0(t) = \int_{\frac{\pi}{6}}^{\frac{\pi}{2}} \frac{sin(w_i t) - sin\left(w_i t - \frac{2\pi}{5}\right) - \sqrt{5}M}{sin(w_i t) - sin\left(w_i t - \frac{2\pi}{5}\right)} dt \quad (4)$$

$$D_0(t)$$
$$= \frac{\int_0^t ((MAX(t) - MIN_0(t) - MAX_0(t) - MIN_0(t))) dt}{\int_0^t (MAX(t) - MIN(t)) dt} \quad (5)$$

$$D_0(t) = \frac{(MAX(t) - MIN_0(t) - V_{sh1}(t)) + V_{sh2}(t)}{MAX(t) - MIN(t)} \quad (6)$$

Only under maximal constant control does the duty cycle remain constant. The others are all time-varying functions. An average shoot-through duty cycle must be established in order to construct the voltage gain equation [39].

$$D_0(t) = \frac{5}{4} - \frac{5\sqrt{5}M}{6} \quad (7)$$

This control strategy's boost factor is established as [36]:

$$B = \frac{1}{\sqrt{\frac{9}{4}M^2 - \frac{15\sqrt{5}}{4}M + \frac{31}{16}}} \quad (8)$$

The voltage conversion ratio, i.e.) the maximal gain of QZSDMC, is calculated using this approach as [40]:

$$G_{mc} = \frac{M}{\sqrt{\frac{9}{4}M^2 - \frac{15\sqrt{5}}{4}M + \frac{31}{16}}} \quad (9)$$

3.1. Conduction losses

The matrix converter losses are discussed as the maximum phase, middle phase and minimum phase
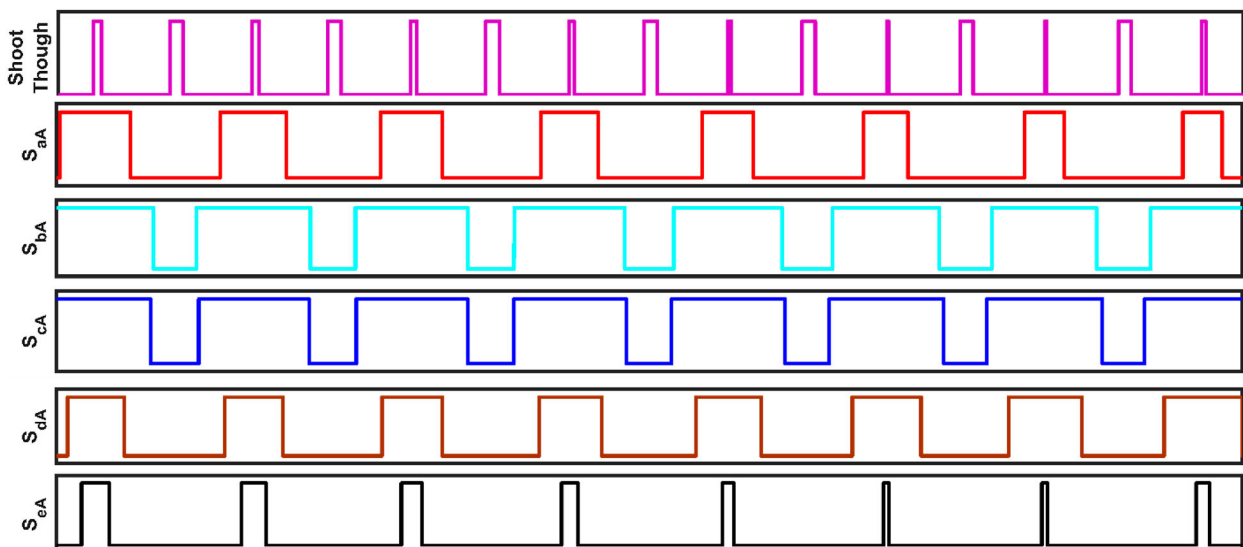

Figure 6. Introduction of shoot-through states in the QZS network.

switches. As the result, it is easy to introduce the conduction loss and the switching loss of the matrix converter. The conduction loss and switching loss are calculated from the measurement value (Vce, ic) and loss data table. In this method, it is easy to analyze the loss of the converter. However, the simulation time is long. In addition, the loss data table is obtained from the datasheet of the switching device or the switching test.

The conduction loss of the maximum phase switch in the matrix converter Pcon_max is expressed by.

$$P_{Con\_max} = \frac{1}{\pi} \int_{\theta_0}^{\pi+\theta_0} D_{max}.V_{on}.i_0 dw_0 t \qquad (10)$$

Where, Dmax is on-duty of the maximum phase switch and Wo is the output angular frequency. In addition, Von, which is the on-state voltage of the device, is calculated by

$$V_{on} = k_{con1}i_0 + k_{con2} \qquad (11)$$

Kcon1 and kcon2 are obtained from the on-state voltage characteristic in the datasheet. The instantaneous value of the load current io is expressed by (12) from the maximum load current Io and the load angle θ0.

$$i_0 = I_0 \sin(w_0 t - \theta_0) \qquad (12)$$

Pcon_max can be calculated from (10). However, It is difficult to derive the loss because Dmax depends on the input current command and the output voltage command. In this paper, the total conduction loss per the output phase Pcon is derived. Consequently, the on-duty command per the output single-phase is expressed as

$$D_{max} + D_{mid} + D_{min} = 1 \qquad (13)$$

where Dmid and Dmin are the on-duties of midium and minimum phase switches. From (13), it can be revealed that only one switch is turned on and two switches are not on-state at same time. Assume that the switching devices with same characteristics are used. Thus, Pcon is expressed by.

$$\begin{aligned} P_{Con\_max} &= \frac{1}{\pi} \int_{\theta_0}^{\pi+\theta_0} D_{max}.V_{on}.i_0 dw_0 t \\ &= \frac{1}{2}k_{con1}I_0^2 + \frac{2}{\pi}k_{con2}I_0 \end{aligned} \qquad (14)$$

3.2. Switching losses

In this section, the turn-on loss of the maximum phase Pton_smax is derived. Consider integral period of each switching loss of the matrix converter. The integral period is different among each switching devices owing to the polar of the output current. The turn-on loss of the maximum phase switch Pton_smax occurs when the polar of the output current io is positive. Additionally, Pton_smax is calculated from the output current and the voltage between the maximum phase and

medium phase (Vmax-Vmid). First, the general turn-on loss is expressed as.

$$P_{SW\_loss} = \frac{1}{T} \int_0^{\frac{T}{2}} \frac{f_s}{V_s} e_{on} v_{sw} dw_0 t \qquad (15)$$

where T is the cycle of io, fs is the switching frequency, Vs is the tested voltage when the switching loss was measured, and Vsw is the drain–source voltage of the device. In addition, the instantaneous turn-on loss eon is expressed by (16).

$$e_{on} = k_{ton1}i_0 + k_{ton2} \qquad (16)$$

Similarly, ktonl and kton2 are obtained from the turn-on loss characteristic in the datasheet. The integral period is used to calculate the switching loss. The integral period is different among each switching devices due to the polar of io. In other words, Pton_smax occurs when the polar of io is positive. Furthermore, the drain–source voltage Vsw is different among each switching devices. Assume that the switching pattern is that the middle phase is certainly gone through. Accordingly, the drain–source voltage of Smax is differential voltage (Vmax – Vmid) between the maximum phase voltage Vmax and the middle phase voltage Vmid. Thus, Pton_smax is expressed by (17).

$$P_{ton\_smax} = \frac{3f_s V_{in}}{2\pi^2 V_s} (2k_{ton1}I_0 + k_{ton2}\pi) \qquad (17)$$

Similarly, the middle phase and minimum phase turn-on loss are expressed.

$$\begin{aligned} P_{ton\_smid} &= \frac{3f_s V_{in}}{\pi^2 V_s} (2k_{ton1}I_0 + k_{ton2}\pi) \\ P_{ton\_smin} &= \frac{3f_s V_{in}}{2\pi^2 V_s} (2k_{ton1}I_0 + k_{ton2}\pi) \end{aligned} \qquad (18)$$

Based on these formulas such as (14) and (17), it is easy to design the matrix converter in terms of efficiency and reduced size. It is noted that the design method depends on the priority of the high efficiency or high power density. When the matrix converter is designed in terms of high power density, the switching frequency is increased. As the result, the input LC filter becomes smaller. However, the size of the heat-sink is large because the switching loss increases. Further, the switching loss is more dominant than conduction loss. Thus, the switching device, which has small parameters kton1, kton2 is selected in reference to the datasheets.

Accordingly, high power density is obtained even if the switching frequency is increased. This is because the volume of heat-sink can be reduced owing to lower switching loss. On the other hand, when the matrix converter is designed in terms of high efficiency, the conduction loss is dominated owing to lower switching frequency. For this reason, the switching device, which has small parameters kcon1, kcon2 is selected from the datasheet. As the result, high efficiency can be obtained because conduction loss is low. Besides, the switching

device in the matrix converter can be selected from the efficiency, which is required in an application.

First, the circuit specification such as the rated power, rated voltage, rated current, and switching frequency is arbitrarily determined. Second, the on-state voltage parameters kcon1, kcon2 and switching loss parameters kton1, kton2, that the demanded efficiency is obtained, are calculated by using (14) and (17). Next, based on the calculated parameters, the switching device is selected from the datasheet. Finally, the efficiency in experiment agrees with that of the design value when the matrix converter is manufactured by using the selected device.

4. Modulation scheme validation using MATLAB/Simulink

The maximum constant boost current controlled PWM technique has been implemented in a five to three-phase QZSDMC. Simulation experiments have been carried out to explore the converter's functionality and behaviour across its complete operational spectrum. The proposed modulation scheme demonstrates excellent performance in all operating regions. The simulation was created in the MATLAB/Simulink environment with the sim-power-system toolbox block. The block diagram depiction of the proposed PWM approach is shown in Figure 7. The goal output voltage and input standards maximum, middle, and minimum are inputted into the duty ratio control block to start the PWM operation. Following that, the resulting duty cycle was assessed in relation to a high-frequency TCM. The control algorithm immediately obtains the output waveform rhythm for regulating the voltage of

Table 1. Parameters used in the simulation system.

Parameters	Values assumed
AC input line-to-ground RMS voltage, V_i	100 Volt
AC input voltage frequency, f_i	50 Hz
QZS-network inductance, L	100 µH
QZS-network capacitance, C	10 µF
QZSDMC switching frequency, f_s	5000 Hz
AC output line-to-ground RMS voltage, V_o	99.89 Volt
AC output line current, I_o	4.6 A
AC output voltage frequency, f_o	50 Hz
Modulation index, M	0.8
Simulation step size	10 µsec
R-Load connected to the QZSDMC	1 KΩ
L-Load connected to the QZSDMC	10 mH

output, and the aforementioned control pulse signals are then used to operate the power switches. Specific system characteristics, as stated in Table 1, were used in the context of simulation, and the correct discrete filter components were chosen to achieve the desired simulation results.

Figure 8 illustrates the flowchart detailing the simulation and experimental validation process for the control strategy applied to the QZSDMC. The procedure commences with the establishment of fixed five-phase reference input and three-phase reference output voltages. Following that, the slope of the carrier waveform is computed, as well as the maximum, minimum, and midway values of the three-phase output baseline waveforms. To create modulation signals, the Maximum Constant Boost Current Modulation approach is chosen. The duty ratio and modulation coefficient are calculated using Equations 6 and 7. After that, the control signals for all dual-direction switches are created. A comparison of the actual output voltages with the reference output voltages is done. The power
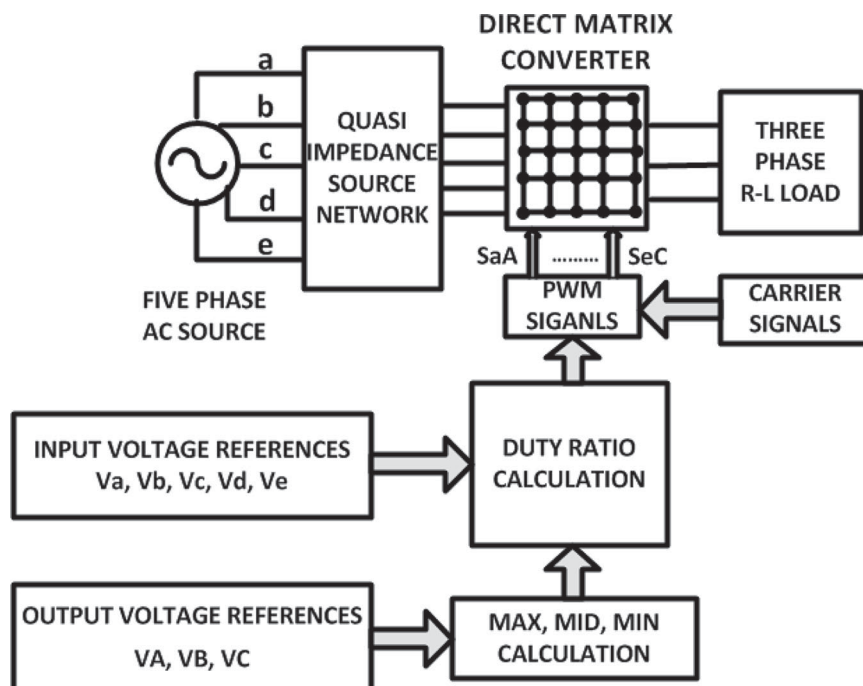

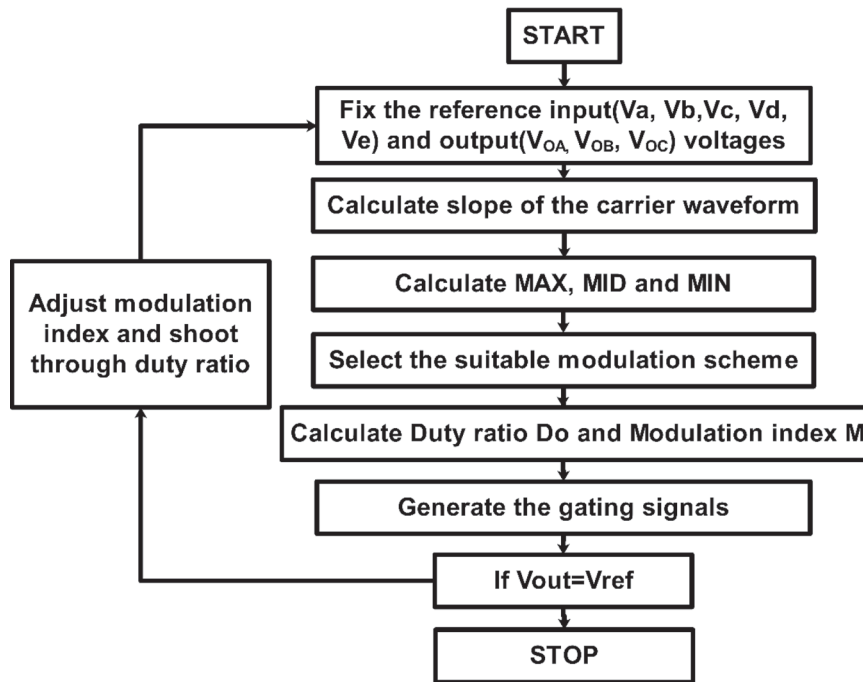**Figure 7.** Block Diagram for the Proposed PWM Method.

Figure 8. Step-by-step procedure involved in maximum constant boost current control PWM technique implemented to five to three-phase QZSDMC.
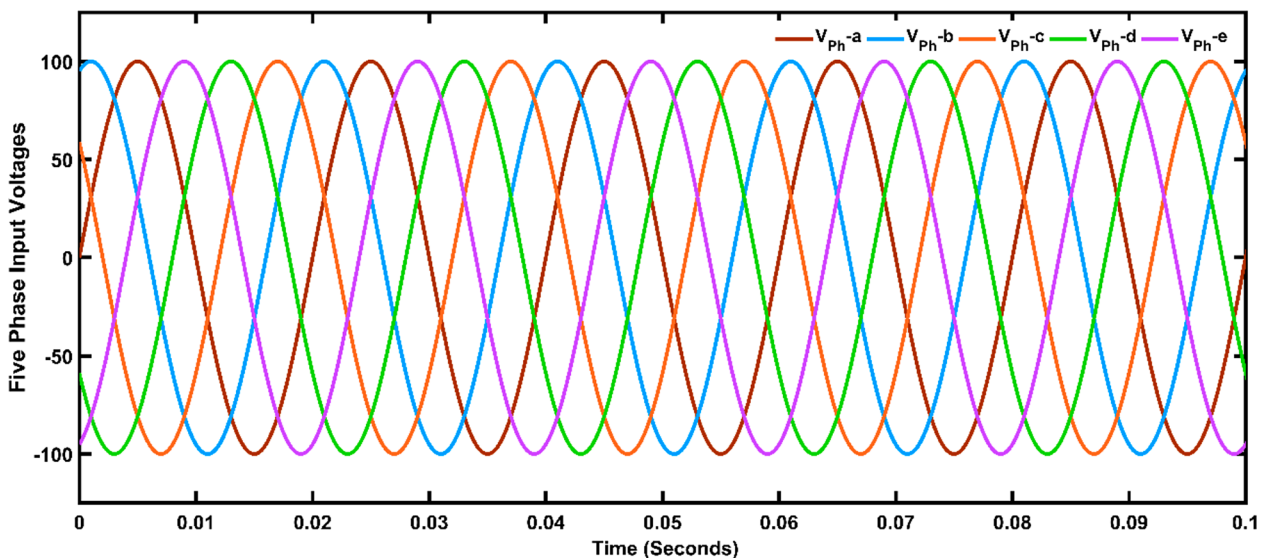

Figure 9. Five-phase input voltages operating at a frequency of 50 Hz.

conversion procedure continues if Vout exceeds Vref. Otherwise, the modulation indices and offset duty ratio are adjusted, with or without common mode furthermore, to improve the five-phase output voltages.

Figure 9 illustrates input voltages of 100 V (peak) and input current of 4.5A supplied to the five-phase to three-phase QZSDMC. The input signals exhibit stability without fluctuations or harmonic content. Furthermore, the input side consistently maintains a unity power factor. To facilitate a clear comprehension of the energy conversion rate, the input voltage is maintained at a constant 100 V in the proposed work.

The Integrated MATLAB function block is used to generate the MATLAB code required for the job. Figures 9–16 show the generated waveforms for input and output properties independently. On the data input side, it's worth noticing that the unified power factor is maintained continuously, as seen in Figure 9. The regulated switching signals provided to the bidirectional control switches are seen in Figure 11. Figures 12–14 show the output voltages and currents of a Maximum Constant boost-controlled five-phase to three-phase QZSDMC running at 50 Hz with a modulation index of 0.8. At a frequency of 50 Hz, the MATLAB simulation provides observed values, especially output three-phase voltages and output load current, measuring 99.89 V and 4.6A.

The voltage Total Harmonic Distortion (THD) and current THD values are shown in Figures 15 and 16 to be 4.03% and 3.76%, respectively, at the operating
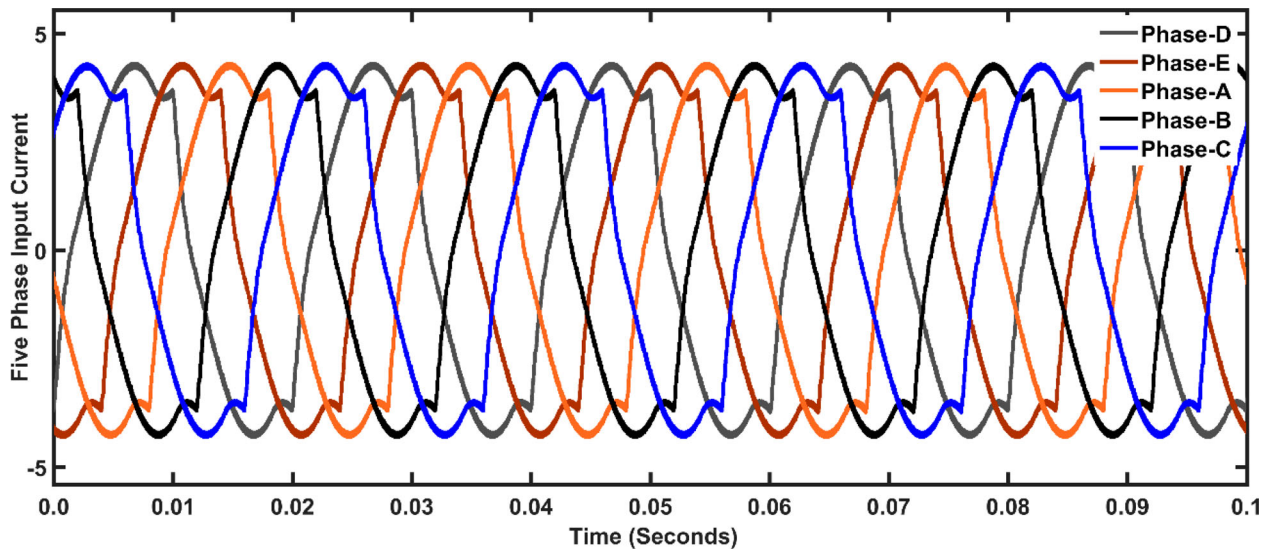
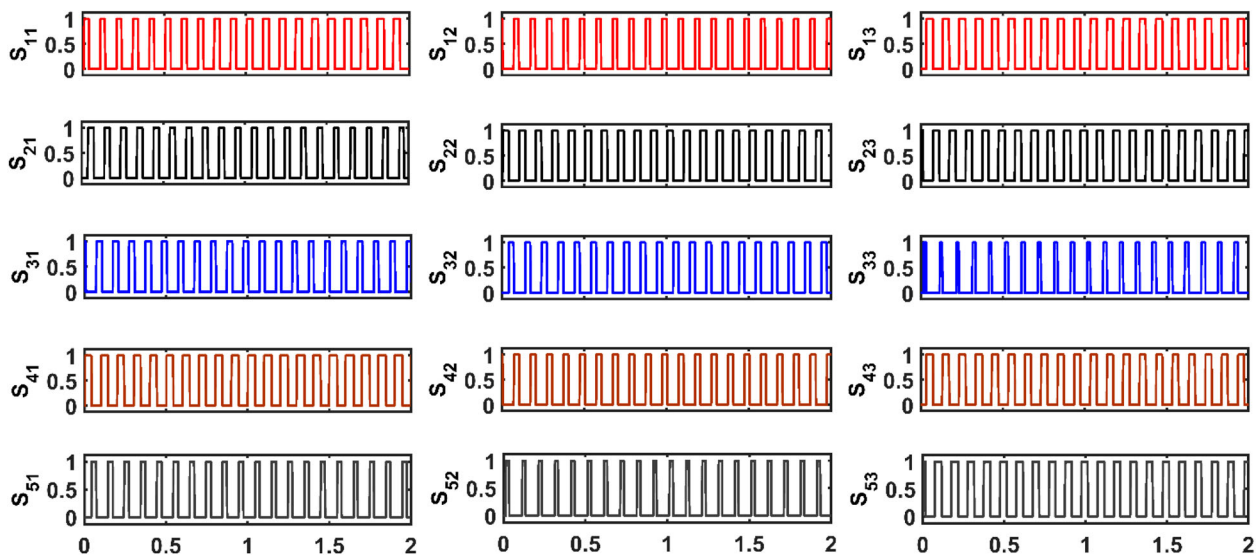**Figure 10.** Five-phase input current operating at a frequency of 50 Hz.

Figure 11. Controlled Gating Signals for Individual Arms.
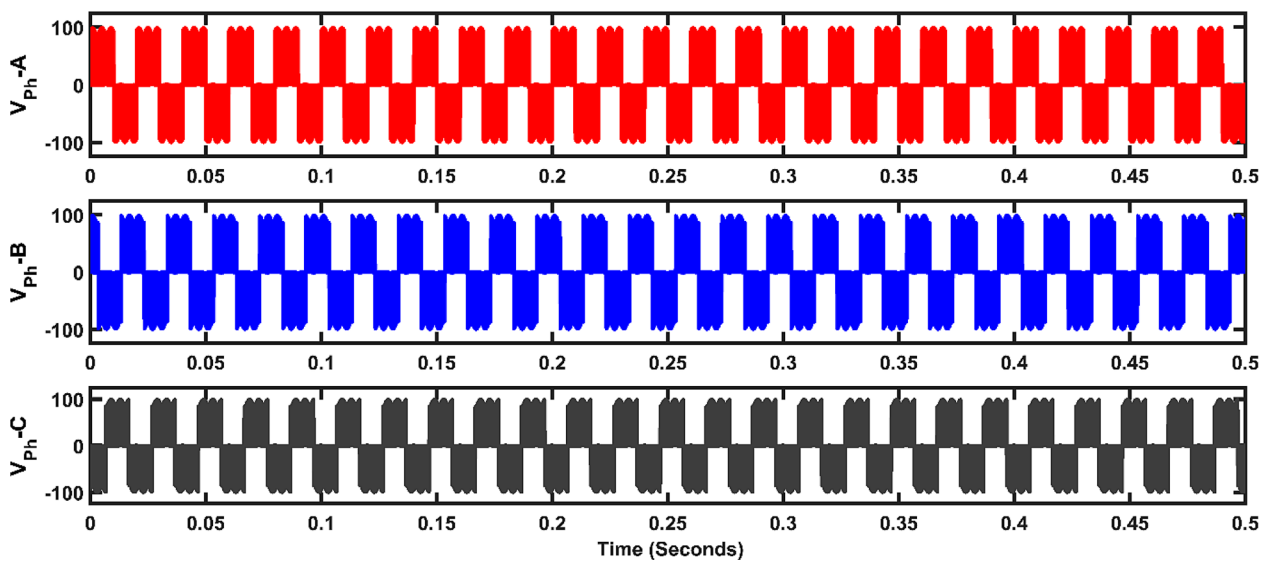

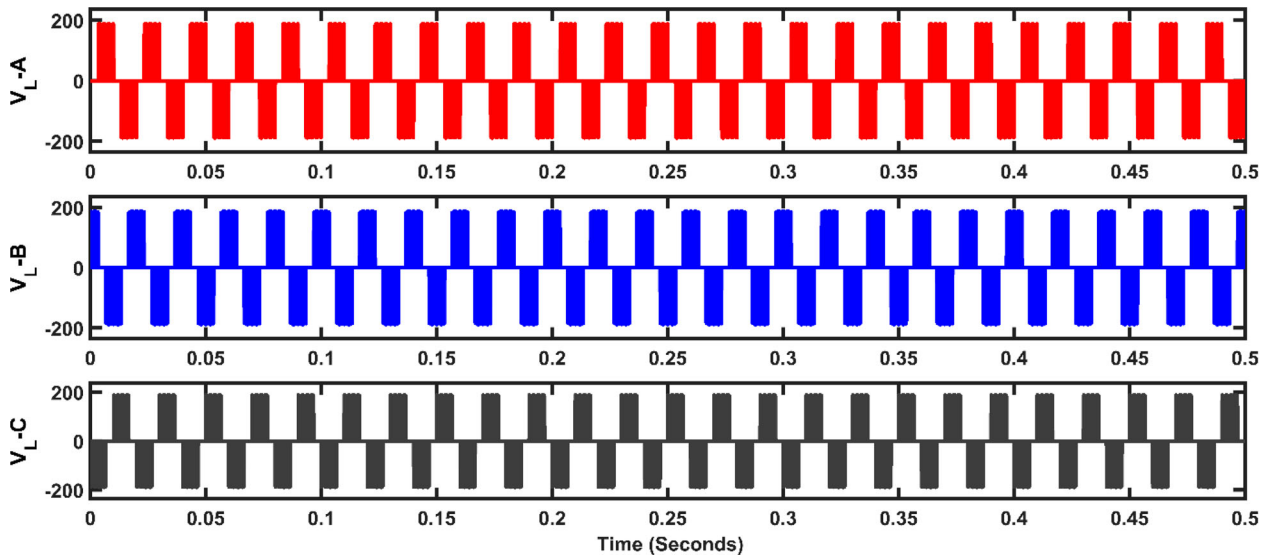**Figure 12.** Output phase voltage in a five to three-phase configuration at a frequency of 50 Hz.

Figure 13. Output line voltage in a five to three-phase configuration at a frequency of 50 Hz.
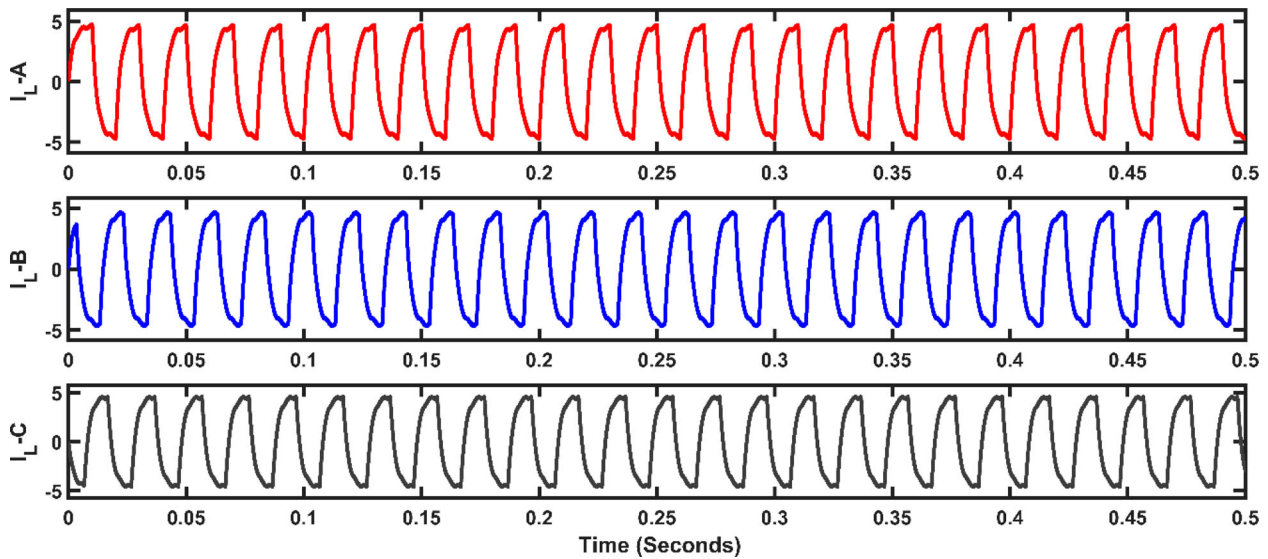

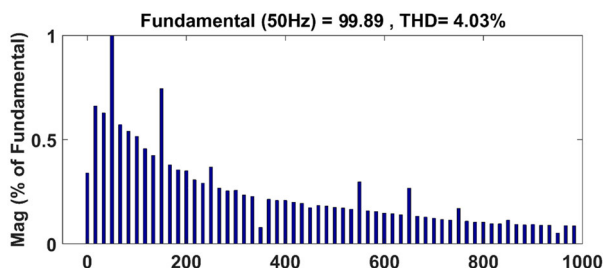**Figure 14.** Output load current in a five to three-phase configuration at a frequency of 50 Hz.

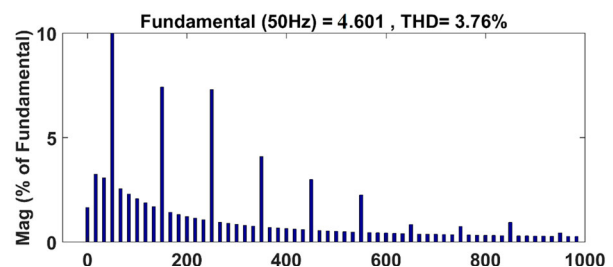**Figure 15.** THD in the output voltages of the five to three-phase QZSDMC.

Figure 16. THD in the output current of the five to three-phase QZSDMC.

frequency of 50 Hz. Notably, these THD values are found to be below the limits set by the IEEE 519-1999 standard. Figures 12–14 underline the maintenance of a unity power factor on the output side, independent of the input power factor. Furthermore, Table 2 provides a comprehensive summary of input and output voltages, input and currents, as well as voltage and current

THDs for five-phase to three-phase systems operating at frequencies of 25, 50, 75, and 100 Hz.

5. Verification by hardware implementation for the proposed QZSDMC

A prototype of the three-to-five-phase QZSDMC has been constructed, and the proposed modulation

Table 2. Output characteristics MCBCC PWM-based QZSDMC at various frequencies.

| Parameters	5φ to 3φ QZSDMC			
	25 Hz	50 Hz	75 Hz	100 Hz
Input voltage(V)	100	100	100	100
Input current(A)	4.5	4.5	4.5	4.5
Output phase voltage(V)	95.15	99.89	97.77	98.89
Output line voltage(V)	191.14	196.88	194.18	198.88
Load current(A)	4.1	4.6	4.4	4.68
Voltage THD %	4.43	4.03	4.30	4.83
Current THD %	4.76	3.76	3.99	3.56

technique has been effectively applied for energy conversion. Figure 17 illustrates the schematic block diagram of the suggested system. New experimental outcomes are utilized to confirm the principles of the maximum constant boost current controlled PWM technique for the five-phase to three-phase QZSDMC. These new experimental findings are instrumental in scrutinizing and affirming the theoretical principles, as well as assessing the consistency and feasibility of digital applications. As a result, the suggested AC-AC converter can be efficiently employed for versatile speed control in multi-phase drive systems.

Figure 17 illustrates the schematic blocks of the experimental setup, while Figure 18 provides a visual representation of the experimental arrangement for the 5φ to 3φ QZSDMC. To establish the necessary experimental prototype configuration, power modules utilizing IXYS-based FIO50-12BD bidirectional switches are utilized. These modules belong to the ISOPLUS i4-PAC series, featuring power diode bridges and power IGBTs that are interconnected diagonally. The IGBTs and diode bridges are designed with a voltage-blocking

capacity of 1200 V, and each unit can accommodate a current of 50A.

This module is readily accessible as a solitary integrated chip featuring five output connectors. Across these five output connectors, four are exclusively allocated for power diode bridges, while one serves the purpose of the IGBT gate drive circuit. A single-chip module, operated by a solitary control signal, can effectively manage the bidirectional current flow. The QZSDMC is equipped with 27 bidirectional power switches, but only 18 of them are effectively utilized. Control signals for the bidirectional switching components are generated using a Spartan three-a digital signal process controller and an Xilinx. The FPGA(XC3SD1800A) board is equipped with logic gates, analog-to-digital and digital-to-analog translation processors, a gate driver, and a core processor. This electronic board can manage PWM signals with frequencies of up to 50.

Damping diode circuits are implemented to protect the entire power module circuit. An autotransformer is employed to furnish the input power supply, delivering 100 V, 50 Hz, 5-phase AC power. The bidirectional switches within the QZSDMC function at a switching frequency of 5 KHz. Table 1 provides a comprehensive overview of the input terminal, filter, and load parameters on the output terminal. In Figures 9 and 10, the input voltage and current provided to the 5φ to 3φ QZSDMC are displayed, along with the resulting output voltage and current waveforms at the fundamental frequency of 50 Hz. Figures 19–21 show the resulting output phase voltage, line voltage, load current, and all five-phase output voltage waveforms for the same fundamental frequency of 50 Hz.
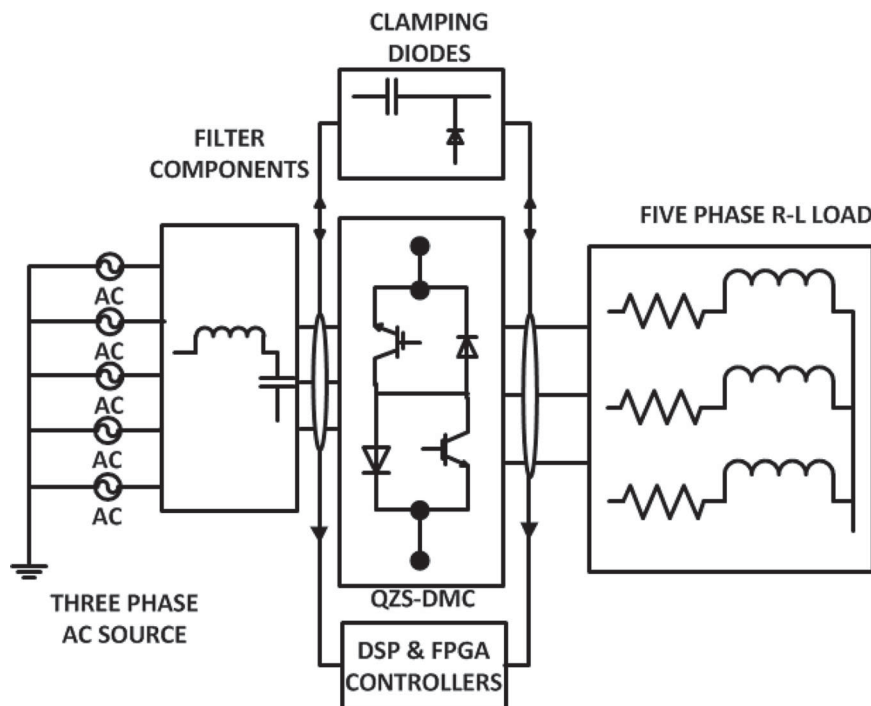
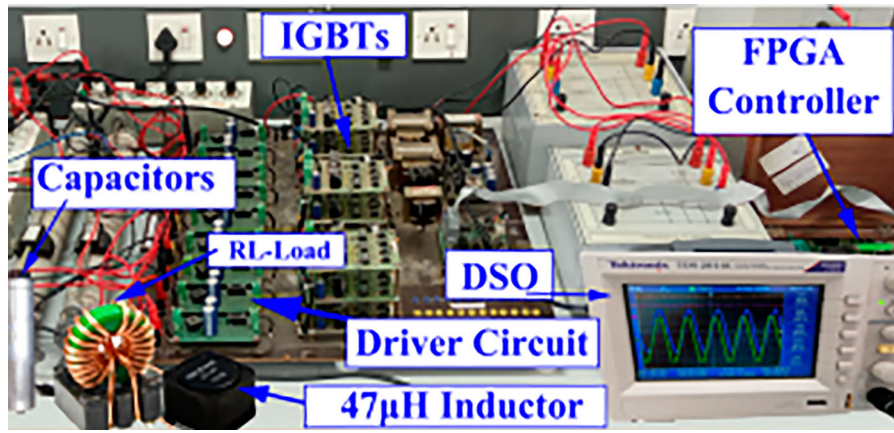**Figure 17.** Schematic block diagram illustrating the proposed system.

Figure 18. Experimental configuration for the five-phase to three-phase quasi-Z-source direct matrix converter.
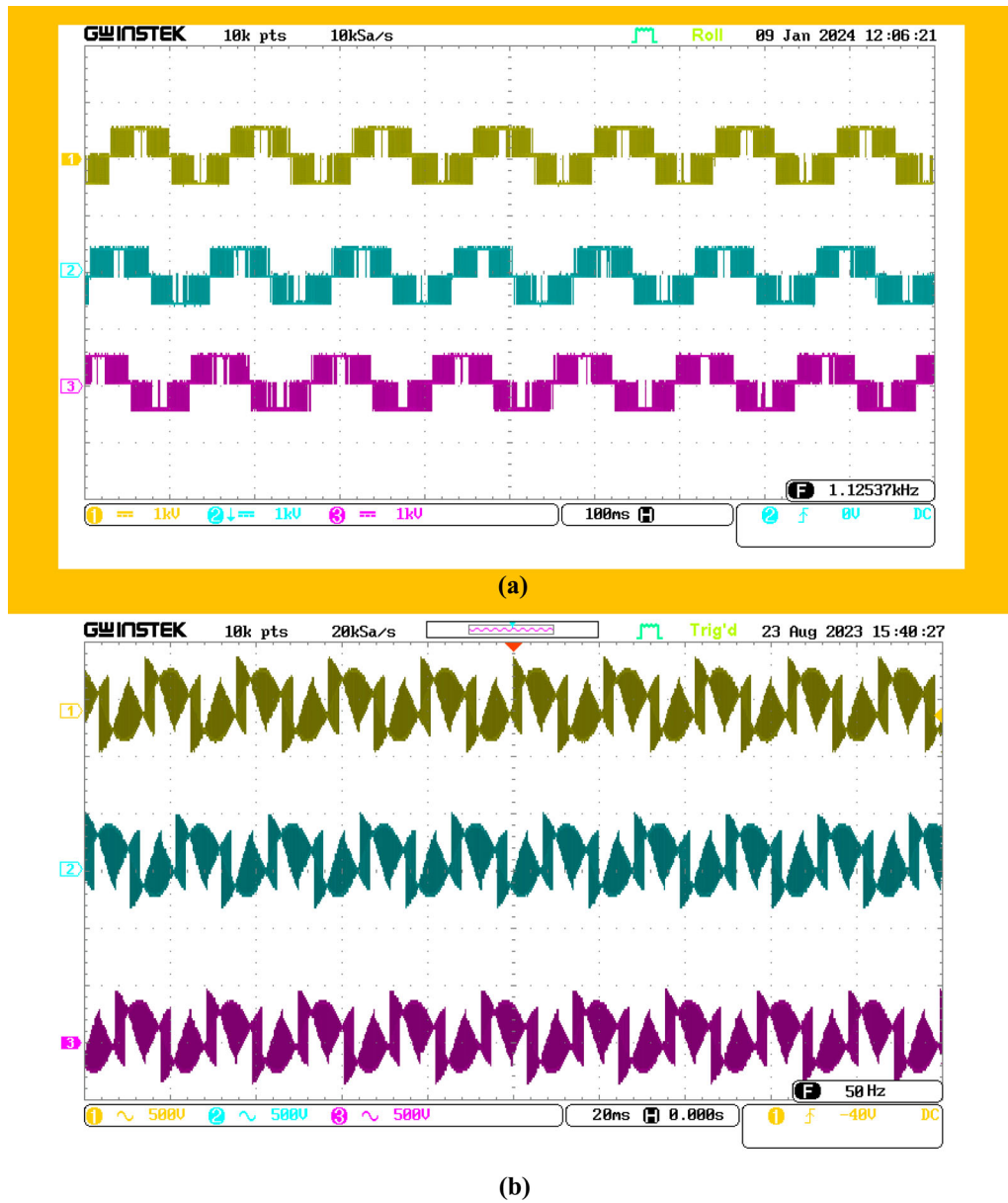

Figure 19. (a) Three phase output phase voltages from 5φ to 3φ QZSDMC. (b) Three phase output phase voltages from 3φ to 3φ QZSDMC.
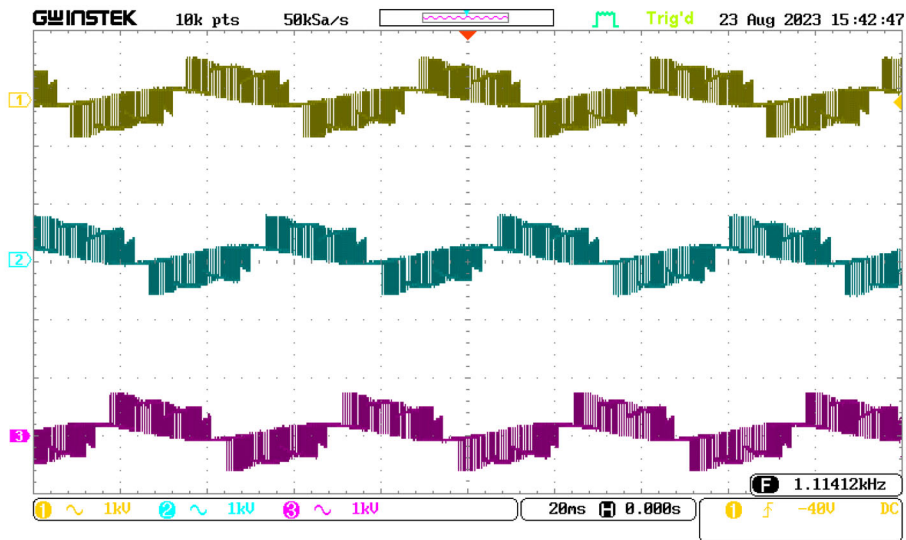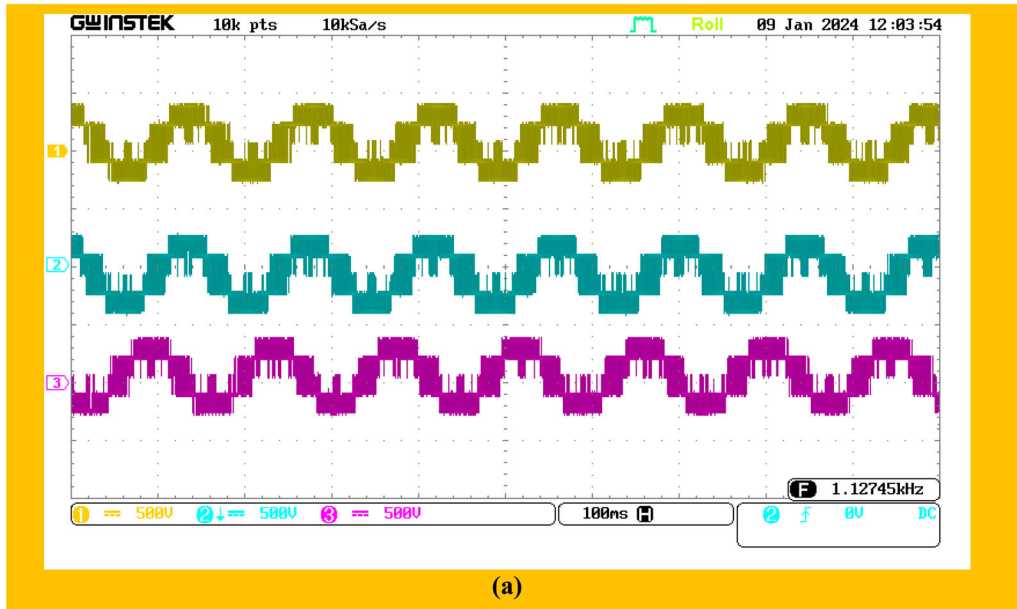
Figure 20. (a) Three-phase output line voltages from 5φ to 3φ QZSDMC. (b) Three-phase output line voltages from 3φ to 3φ QZSDMC.

In general, Figures 19–21 display the investigational measurements of the phase output, line voltage, and load current of the 5φ to 3φ QZSDMC at an operating frequency of 50 Hz. When compared to the conventional DMC, as shown in Figure 2, the practical results reveal that the 5φ to 3φ QZSDMC achieves a superior voltage gain. The elevated voltage gain is attributed to the uniform dispersal of shoot-through states while keeping the active conditions intact. Figures 22 and 23 demonstrate that the phase voltage of output patterns is precisely synchronized with the output load currents, signifying the preservation of a UPF at the load end.

Therefore, the experimental outcomes of the QZS-DMC, utilizing the maximum constant boost current controlled modulation technique, confirm its superior performance compared to conventional DMC systems.

Figure 8 presents a flowchart outlining the step-by-step process for validating the experiment. The application of the maximum constant boost current control method for the 5φ to 3φ QZSDMC is thoroughly presented. Table 3 provides a comparative analysis, contrasting the simulated outcomes with the experimental prototype findings. Many of the measured outcomes closely match the theoretical results derived from the simulation. However, some discrepancies arise due to the non-ideal parameters of inductors and capacitors in the experimental setup. From the result, unanticipated voltage dissipation takes place to overpower components and inductors, resulting in measured QZS network output voltages that are lower than the simulated values, along with observed disparities in current levels.

The experimental findings exhibit a high degree of correspondence with the simulated results, indicating
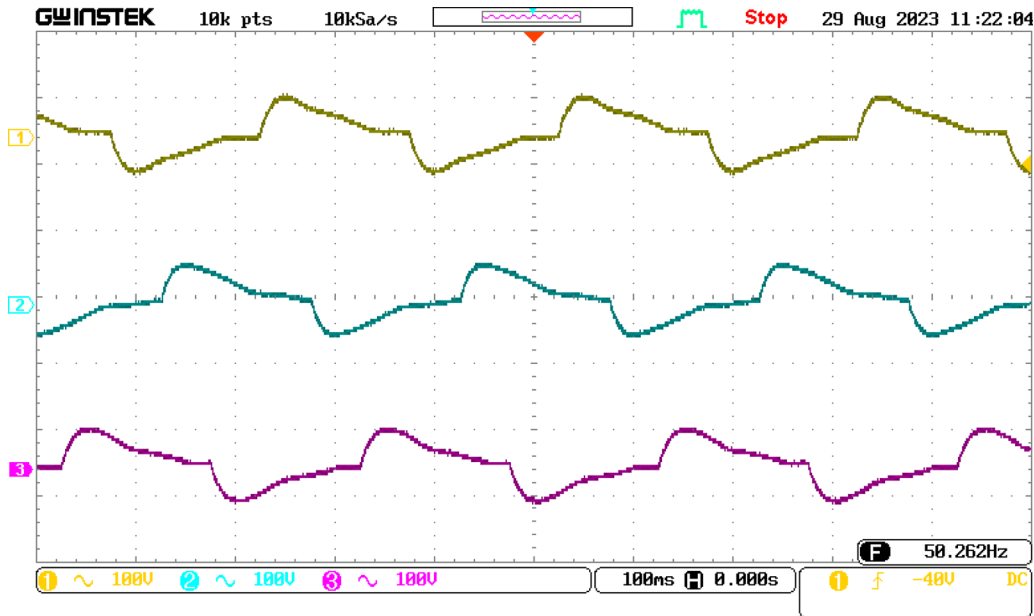
(a)
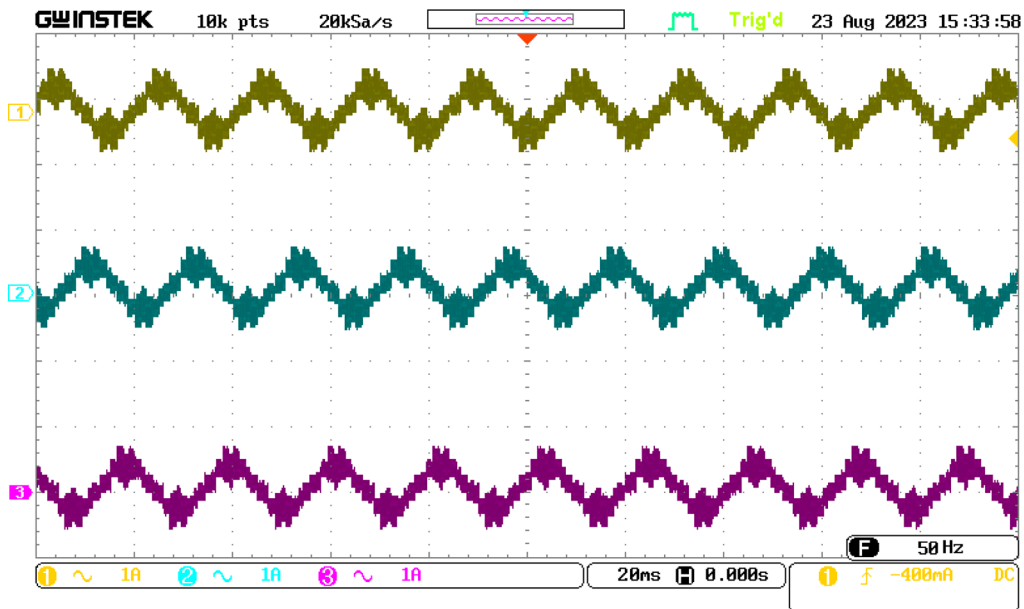
**(b)**

Figure 21. (a) Three phase output load currents from 5φ to 3φ QZSDMC. (b) Three phase output load currents from 3φ to 3φ QZSDMC.

a robust agreement between them. Figures 22 and 23 provide visual representations of the Total Harmonic Distortions (THDs) for output voltage and output current. The 5φ to 3φ QZSDMC demonstrates Total Harmonic Distortions (THDs) of 5.3% for voltage waveform and 3.6% for current waveform. On the other hand, the THDs for the five-phase input voltage and current are 4.03% and 3.76%, respectively. These findings showcase the enhanced presentation of the 5φ to 3φ QZSDMC when utilizing the suggested maximum constant boost current control PWM approach. Moreover, on the input terminal, the current waveform aligns with the voltage waveforms, illustrating the converter's

capability to uphold a unity power factor. The prototype module employs bidirectional switches, providing the benefit of requiring a reduced count of IGBT switches for multi-phase functionality. Nevertheless, it is associated with significant drawbacks, including increased conduction losses, a two-step commutation process, the necessity for additional line inductance to ensure safe operation, current during the switching process, and the requirement for additional circuits to handle dead time compensation.

The switching losses and efficiency of the existing traditional AC to AC power converters are 109.4W and 95.4%. Table 4 represents the switching losses, total
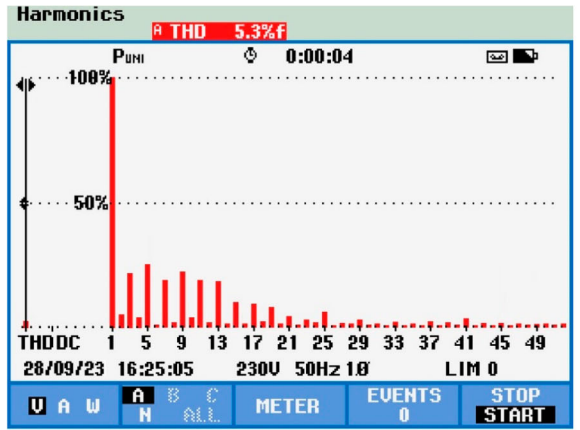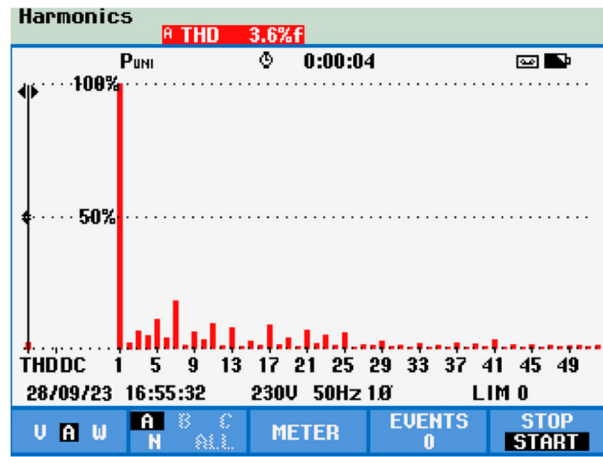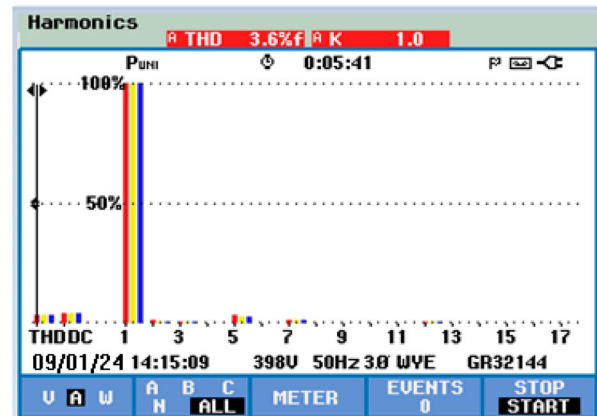
(a)
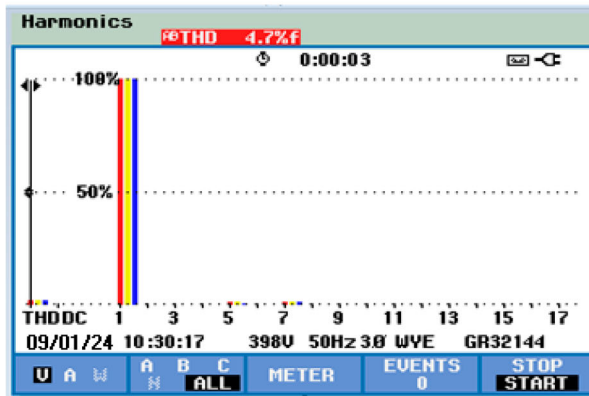
(b)

Figure 22. (a) Per phase output voltage THD from 5φ to 3φ QZSDMC at the frequency of 50 Hz. (b) Per phase output voltage THD from 3φ to 3φ QZSDMC at the frequency of 50 Hz.

(a)

(b)

Figure 23. (a) Per phase load current THD from 5φ to 3φ QZSDMC at the frequency of 50 Hz. (b) Per phase load current THD from 3φ to 3φ QZSDMC at the frequency of 50 Hz.

losses in the circuit, and efficiency of the proposed converter with various modulation control schemes. The maximum efficiency of 83.3% and minimum switching loss of 105W have been achieved by the proposed QZSDMC using the maximum voltage gain control technique. The addition of passive components and the operating switch's availability in the proposed converter increased as a result of switching losses decreased and the efficiency reduced.

The testing of developed QZSDMC is done over a wide range of fundamental frequencies. Table 5 shows the comparison of ZSDMC, discontinuous, and continuous QZSDMC AC–AC converter topologies. From the comparison, it is ensured that the QZSDMC offers a high voltage boost ratio, good wave-form quality, lesser capacitor voltage stress, and continuous input current. The simulation and the investigational results of the prototype verify the feasibility of the suggested QZSDMC topology and its control strategy. Comparing the hardware results with the simulation results that show the proposed modulation scheme for QZS-DMC provides better results at all the fundamental frequencies.

6. Conclusion

This research paper introduces a novel PWM technique for the QZSDMC. The proposed PWM scheme is based on the maximum boost current control PWM method, making it easily implementable in real time. Implementing this modulation scheme in conjunction with the QZSDMC effectively mitigates the constraints associated with conventional DMCs. Conventional DMC faces limitations due to its restricted voltage transfer ratio, a challenge that is successfully overcome by the QZSDMC. The QZSDMC enables the generation of sinusoidal output voltages across a wide range of frequencies without any frequency limitations, providing versatility in frequency output. The proposed control scheme for the QZSDMC enhances the applicability of DMC across various industries, broadening its potential applications in wind energy conversion systems. The maximum boost current control-based QZSDMC efficiently delivers power to a wide range of industrial loads. The proposed converter as well as the modulation technique produces the maximum voltage transfer ratio of 1.05. The output voltage gain reached

Table 3. comparative analysis between the results obtained from simulation and experimentation of the 5φ to 3φ QZSDMC.

Parameters of QZSDMC	Simulated results	Experimental results
Input phase voltage (V) (effective voltage)	100	100
Input current (Amperes)	4.5	4.2
Output phase voltage (V) (effective voltage)	99.89	97.3
Output line voltage (V) (effective voltage)	196.88	192.8
Output current (Amperes)	4.6	4.9
Voltage boost factor	1.99	1.91
Shoot-through duty cycle	0.34	0.34
Output voltage gain	2.01	1.99
Voltage THD	4.03	5.3
Current THD	3.76	3.6

nearly 1.99 compared with the traditional power converters. The voltage THD and current THD are maintained within the acceptable limit of 5.3 and 3.6 respectively. The power factor have been maintained nearly unity throughout the all mode of operations. Additionally, the suggested converter, along with its control system, can function effectively under its esteemed load condition, even when equipped with simple QZS circuit components. In contrast to traditional DMC, the QZSDMC based on maximum boost current control experiences fewer commutation problems because the QZS network eliminates the necessity for dead time. Furthermore, the QZSDMC necessitates fewer switches and can execute both buck and boost operations efficiently using this streamlined switch configuration. The proposed QZSDMC circuit offers several key benefits compared to traditional DMC.

These advantages encompass enhanced reliability under abnormal operating conditions, improved efficiency, stable output regulation, cost-efficiency,

diminished commutation effects, and heightened voltage gain. Quasi-Z-source direct matrix converters (qZSDMCs) are a type of power converter that combine the benefits of quasi-Z-source inverters and direct matrix converters. While they offer several advantages, such as improved voltage gain, higher efficiency, and better power quality, they also have some disadvantages. Here are the key disadvantages of quasi-Z-source direct matrix converters are Complex Control Algorithms: The control strategies for qZSDMCs are more complex compared to traditional converters. Implementing these control algorithms requires sophisticated digital signal processing and can be challenging, increasing the development and operational complexity. Increased Component Count: qZSDMCs typically require more components, including inductors, capacitors, and switching devices, compared to conventional direct matrix converters. This leads to higher costs, larger size, and increased potential points of failure. Higher Initial Cost: Due to the increased number of components and the complexity of the control system, the initial cost of implementing qZSDMCs is higher. This can be a significant disadvantage in cost-sensitive applications. Complex Design and Integration: The design and integration of quasi-Z-source networks into the matrix converter topology are more complex. This complexity can result in longer design cycles and require more advanced engineering expertise. Electromagnetic Interference (EMI): The high switching frequencies and complex switching patterns can lead to increased electromagnetic interference (EMI), which necessitates additional filtering and shielding measures, further adding to the cost and complexity. Thermal Management Issues: The increased number of active and passive components generates more heat, which

Table 4. Loss and Efficiency comparison of the proposed QZSDMC.

Control techniques	Input power (kW)	Switching losses (W)	Total losses (W)	Output power (kW)	Efficiency (%)
Simple maximum boost control	1.5	121	185	1.194	79.6
Maximum boost control	1.5	116	179	1.205	80.3
Maximum constant boost control	1.5	110	166	1.224	81.6
Maximum voltage gain control	1.5	105	145	1.250	83.3
Hybrid minimum voltage stress control	1.5	111	157	1.232	82.1

Table 5. Quantitative comparison of direct and in-direct QZSDMC with discontinuous and continuous mode operations.

Parameters	ZSDMC	Discontinuous QZSDMC	Continuous QZSDMC	Discontinuous QZSIDMC	Continuous QZSIDMC
Total number of inductors and capacitors required	09	15	12	27	27
Additional input LC	Yes	Yes	No	Yes	No
Ripples in Current	High	Low	Low	Low	Low
Ripples in Voltage	Low	High	Medium	High	Medium
Stresses in the Inductor current	Low	High	Medium	High	Medium
Stresses in Capacitor voltage	Medium	Low	High	Low	High
Gain	Low	High	High	High	High
THD of input current	Medium	High	Low	High	Low
THD of output voltage	High	Medium	Low	Medium	Low
Required current rating of element	Low	High	Medium	High	Medium
Required voltage rating of the element used	Medium	Low	High	Low	High
Losses	Medium	High	Low	High	Low
Efficiency	High	Low	High	Low	High

poses thermal management challenges. Effective cooling solutions are required to maintain reliable operation, impacting the overall design and cost. Reliability Concerns: With more components and a more complex control strategy, the reliability of qZSDMCs can be a concern. Each additional component is a potential point of failure, and the increased complexity of the system can make troubleshooting and maintenance more difficult. Limited Commercial Availability: As an emerging technology, quasi-Z-source direct matrix converters are not as widely available or as mature as more traditional converter technologies. This can limit their adoption in industrial applications and make it harder to find experienced personnel and support. Efficiency at Low Load Conditions: While qZSDMCs can achieve high efficiency at rated load, their efficiency can drop significantly at low load conditions. This is due to the losses in the passive components and the complex control required to maintain proper operation under varying loads.

Despite these disadvantages, quasi-Z-source direct matrix converters are a promising technology for applications requiring high reliability, compact size, and improved power quality. However, addressing these drawbacks is crucial for their broader adoption and deployment in various industrial and commercial applications. The suggested modulation scheme is verified through MATLAB simulation, and its implementation has been further validated through hardware testing.

Disclosure statement

No potential conflict of interest was reported by the author(s).

ORCID

Soundarapandiyan Manivannan http://orcid.org/0000-0001-6490-0524

References

[1] Ghaderi D, Padmanaban S, Maroti PK, et al. Design and implementation of an improved sinusoidal controller for a two-phase enhanced impedance source boost inverter. Comput Electr Eng. 2020;83:106575. ISSN 0045-7906. doi:10.1016/j.compeleceng.2020.106575

[2] Ye Y, Chen M, Wang X, et al. Boost-type common-ground PV inverter based on quasi-Z-source and switched-capacitor. Int J Electr Power Energy Syst. 2023;144:108522. ISSN 0142-0615. doi:10.1016/j.ijepes.2022.108522

[3] Veerachary M, Kumar P. Analysis and design of quasi-Z-source equivalent DC–DC boost converters. IEEE Trans Ind Appl. Nov–Dec 2020;56(6):6642–6656. doi:10.1109/TIA.2020.3021372

[4] Shen H, Zhang B, Qiu D. Hybrid Z-source boost DC–DC converters. IEEE Trans Ind Electron. Jan 2017;64(1):310–319. doi:10.1109/TIE.2016.2607688

[5] Junjun L, Daiwei T, Bowei X, et al. Double-integral sliding mode control of the switched-inductor quasi-Z source boost converter. Meas Control. 2023;56(3–4):507–517. doi:10.1177/00202940221110936

[6] Naderi S, Rastegar H. A new non-isolated active quasi Z-source multilevel inverter with high gain boost. IEEE Access. 2023;11:2941–2951. doi:10.1109/ACCESS.2023.3234040

[7] Qi Q, Ghaderi D, Guerrero JM. Sliding mode controller-based switched-capacitor-based high DC gain and low voltage stress DC-DC boost converter for photovoltaic applications. Int J Electr Power Energy Syst. 2021;125:106496. ISSN 0142-0615. doi:10.1016/j.ijepes.2020.106496

[8] Shigeuchi K, Xu J, Shimosato N, et al. A modulation method to realize sinusoidal line current for bidirectional isolated three-phase AC/DC dual-active-bridge converter based on matrix converter. IEEE Trans Power Electron 2020;36(5):6015–6029. doi:10.1109/TPEL.2020.3026977

[9] Waghmare MA, Umre BS, Aware MV, et al. Dual stage single-phase to multiphase matrix converter for variable frequency applications. IEEE Trans Power Electron 2022;38(2):1372–1377. doi:10.1109/TPEL.2022.3207515

[10] Maheswari KT, Bharanikumar R, Bhuvaneswari S. Review on matrix converter topologies for adjustable speed drives. Int J Innov Technol Explor Eng. 2019;8(5):53–57.

[11] Thangavel MK, Ramasamy BK, Ponnusamy P. Performance analysis of dual space vector modulation technique-based quasi Z-source direct matrix converter. Electr Power Components Syst. 2020;48(11):1185–1196. doi:10.1080/15325008.2020.1834018

[12] Guo M, Liu Y, Ge B, et al. Dual, three-level, quasi-Z-source, indirect matrix converter for motors with open-ended windings. IEEE Trans Energy Convers 2022;38(1):64–74. doi:10.1109/TEC.2022.3187419

[13] Xu Y, Wang Z, Zou Z, et al. Voltage-fed isolated matrix-type AC/DC converter for wind energy conversion system. IEEE Trans Ind Electron 2022;69(12):13056–13068. doi:10.1109/TIE.2022.3140524

[14] Xu Y, Wang Z, Liu P, et al. The modular current-fed high-frequency isolated matrix converters for wind energy conversion. IEEE Trans Power Electron 2021;37(4):4779–4791. doi:10.1109/TPEL.2021.3123204

[15] Liao K, Lu D, Wang M, et al. A low-pass virtual filter for output power smoothing of wind energy conversion systems. IEEE Trans Ind Electron 2022;69(12):12874–12885. doi:10.1109/TIE.2021.3139177

[16] Ramalho AWS, Vitorino MA, Corrêa MBdR, et al. New family of two-to-three-phase AC–AC indirect matrix converters with open-end rectifier stage. IEEE Trans Ind Appl 2021;58(1):517–530. doi:10.1109/TIA.2021.3128369

[17] Alizadeh M, Kojuri SS. Modelling, control, and stability analysis of quasi-Z-source matrix converter as the grid interface of a PMSG-WECS. IET Gener Transm Distrib 2017;11(14):3576–3585. doi:10.1049/iet-gtd.2017.0178

[18] Hakemi A, Monfared M. Very high gain three-phase indirect matrix converter with two Z-source networks in its structure. IET Renew Power Gener 2017;11(5):633–641. doi:10.1049/iet-rpg.2016.0368

[19] Manivannan S, Saravanakumar N, Vijeyakumar KN. Three-phase power conversion using quasi Z source direct matrix converter (QZSDMC) for fixed frequency to variable frequency using direct duty ratio based pulse width modulation technique. Int J Electron. 2022;109(7):1184–1213. doi:10.1080/00207217.2021.1966668

[20] Manivannan S, Saravanakumar N, Vijeyakumar KN. Three-phase to K-phase power conversion using voltage fed quasi Z source direct matrix converter with maximum constant boost control technique. Electr Eng. 2022;104:3603–3617. doi:10.1007/s00202-022-01572-x

[21] Manivannan S, Saravanakumar N, Vijeyakumar KN. Dual space vector PWM technique for a three-phase to five-phase quasi Z-source direct matrix converter. Automatika. 2022;63(4):756–778. doi:10.1080/0005 1144.2022.2078945

[22] Manivannan S, Rajalashmi K, Saravanakumar N. DDR-Based PWM technique for fixed frequency three-phase to variable frequency K-phase power conversion using QZSDMC. J Eng Res. 2023. ISSN 2307-1877. doi:10.1016/j.jer.2023.11.003

[23] Sofiane O, Hatem G, Tahar B. Robust control of an associated PMSG-Matrix converter wind plant. In 2019 1st International Conference on Sustainable Renewable Energy Systems and Applications (ICSRESA); Tebessa, Algeria; 2019. p. 1–5. doi:10.1109/ICSRESA49121. 2019.9182479

[24] Singh U, Rizwan M. Analysis of wind turbine dataset and machine learning based forecasting in SCADA-system. J Ambient Intell Humaniz Comput. 2023;14: 8035–8044. doi:10.1007/s12652-022-03878-x

[25] Sengar S, Liu X. Ensemble approach for short term load forecasting in wind energy system using hybrid algorithm. J Ambient Intell Humaniz Comput. 2020;11: 5297–5314. doi:10.1007/s12652-020-01866-7

[26] Vidhya DS, Venkatesan T. Quasi-Z-source indirect matrix converter fed induction motor drive for flow control of dye in paper mill. IEEE Trans Power Electron. 2018. doi:10.1109/TPEL.2017.2675903

[27] Krishnan S, Umasankar P, Mohana P. A smart FPGA based design and implementation of grid connected direct matrix converter with IoT communication. Microprocess Microsyst. 2020. 76:103107. doi:10.1016/ j.micpro.2020.103107

[28] Khan IA, Flah A, Agarwal A, et al. Trapezoidal modulated direct matrix converter: for higher frequency AC/AC conversion. Indian J Pure Appl Phys. 2021;59:211–215.

[29] Zahra M, Jafari M, Zhu J, et al. Bidirectional power flow control with stability analysis of the matrix converter for microgrid applications. Int J Electr Power Energy Syst. 2019;110:725–736. doi:10.1016/j.ijepes.2019. 03.053

[30] Pipolo S, Formentini A, Trentin A, et al. A novel matrix converter modulation with reduced number of commutations. IEEE Trans Ind Appl. 2021: 1. doi:10.1109/TIA.2021.3087121

[31] Sayed MA, Iqbal A. Simple PWM technique for a three-to-five phase matrix converter. Int Trans Electr Energ Syst. 2021;31:12860. doi:10.1002/2050-7038.12860

[32] Varajão D, Esteves Araújo R. Modulation methods for direct and indirect matrix converters: a review. Electronics (Basel). 2021;10(7):1–29. doi:10.3390/elec tronics10070812

[33] Rasappan SK, Williams RB, Muthusamy S, et al. A novel ultra sparse matrix converter as a power transferring device for gearless wind energy conversion systems based on renewable energy applications. Sustainable Energy Technol Assess. 2022;50:101830. doi:10.1016/j.seta.2021.101830

[34] Palma L. A quasi Z-source matrix microinverter for grid connected PV applications. In: 2020 International Symposium on Power Electronics, Electrical Drives, Automation and Motion (SPEEDAM); 2020 Jun. p. 526–531. doi:10.1109/SPEEDAM48782.2020.9161972

[35] Chanekar S, Pandit S, Shet VN. Matrix converter: technology and application. J Electr Eng Electron Des (e-ISSN: 2584-0959). 2023;1(1):21–30. doi:10.48001/ joeeed.2023.1121-30

[36] Bento A, Paraíso G, Costa P, et al. On the potential contributions of matrix converters for the future grid operation, sustainable transportation and electrical drives innovation. Appl Sci. 2021;11:4597.

[37] Liu Y, Abu-Rub H. Interactive grid interfacing system by matrix-converter-based solid state transformer with model predictive control. IEEE Trans Ind Inform. 2020;16:2533–2541. doi:10.1109/TII.2017.2679137

[38] Mir TN, Singh B, Bhat AH. Improvised multi-objective model predictive control of matrix converter using fuzzy logic and space vectors for switching decisions. IET Power Electron. 2020;13:758–764. doi:10.1049/ iet-pel.2018.5873

[39] Lei J, Feng S, Wheeler P, et al. Steady-state error suppression and simplified implementation of direct source current control for matrix converter with model predictive control. IEEE Trans Power Electron. 2020;35:3183–3194. doi:10.1109/TPEL.2019.2928874

[40] Toledo S, Caballero D, Maqueda E, et al. Predictive control applied to matrix converters: a systematic literature review. Energies. 2022;15(20):7801. doi:10.3390/en15207801